European Journal of Soil Science, June 1997, **48**, 213–225

A hard sandy-loam soil from semi-arid Northern Cameroon: I. Fabric of the groundmass

M. LAMOTTE[a], A. BRUAND[b], F.X. HUMBEL[a], A.J. HERBILLON[c] & M. RIEU[d]

[a]*ORSTOM, Département TOA, UR 12, 213 rue La Fayette, 75480 Paris;* [b]*INRA, Unité de Science du sol–SESCPF, Centre de Recherche d'Orléans, Avenue de la Pomme de Pin, 45 160 Ardon;* [c]*CNRS, Centre de Pédologie-Biologie, UPR 6831 du CNRS associée à l'Université H. Poincaré-Nancy I, BP 5, 54 501 Vandœuvre-les-Nancy; and* [d]*ORSTOM, Département DEC, 213 rue La Fayette, 75480 Paris, France*

Summary

In semi-arid tropics soil hardening may reduce both water infiltrability and biological activity, thus inducing the development of large almost bare areas. A sandy-loam soil with contrasting loose and underlying hard horizons was studied in the southern plain of the Chad basin. The fabrics of these horizons were studied using combined sieving and sedimentation techniques, mercury porosimetry and scanning electron microscopy. The horizons had similar particle size distributions of the skeleton grains. The hard horizon differs by a small increase in its fine clay (<0.2 μm) content. The hardness is closely related to a fabric with clay coatings on the skeleton grains and clay wall-shaped bridges linking the latter. This induces a strong continuity of the solid phase. This fabric requires a minimum of clay content (6%) to make the coatings and the wall-shaped bridges, and it can be 30% less porous than the loose horizon, without any change in the packing of the skeleton grains. These characteristics of the fabric of the hard horizon are like those of fragipans elsewhere. The continuity of the solid phase, from the microscopic to the macroscopic scale, as well as the absence of a network of cracks explains the considerable strength of the hard horizon, and consequently the difficulties for water infiltration, root penetration and tillage.

Un sol sablo-limoneux à forte cohésion du Nord-Cameroun: I. Mode d'assemblage des constituants élémentaires

Résumé

Dans les régions tropicales semi-arides, le durcissement des sols limite l'infiltration de l'eau et l'activité biologique, provoquant ainsi le développement de grandes étendues presque désertiques. Un sol sablo-limoneux présentant un horizon meuble au-dessus d'un horizon à forte cohésion a été sélectionné dans le bassin tchadien. L'étude de ces horizons a été réalisée par granulométrie, porosimétrie au mercure et microscopie électronique à balayage. Les deux horizons possèdent une même distribution de taille des grains du squelette. En revanche, l'horizon à forte cohésion se distingue par une faible augmentation de la teneur en argile fine (<0.2 μm) et par le mode d'assemblage de ses constituants élémentaires. Les grains du squelette sont revêtus d'argile et reliés par des cloisons argileuses. Une forte continuité de la phase solide est ainsi obtenue avec un minimum d'argile (6%). La porosité de l'horizon à forte cohésion est de 30% inférieure à celle de l'horizon meuble, sans différence dans l'assemblage des grains du squelette. Les caractéristiques de l'assemblage des constituants élémentaires des sols étudiés présentent de nombreuses similarités avec celles décrites pour des fragipans. Enfin, en l'absence de réseau fissural, la continuité de la phase solide explique la forte cohésion, et consécutivement les difficultés d'infiltration de l'eau, de pénétration racinaire et de travail du sol.

Correspondence: A. Bruand. E-mail: ary.bruand@orleans.inra.fr
Received 27 June 1996; revised version accepted 13 December 1996

Introduction

Soils with dense hard horizons near the surface are common in many parts of the World (FAO–UNESCO, 1975). Their occurrence, probably underestimated because of uncertainties about their identification, is one of the major limitations for soil use, particularly in the semi-arid tropics (Witty & Knox, 1989).

Under the sudano-sahelian climate in the southern plain of the Chad basin hard soils impede infiltration of water, penetration of roots, and tillage. Brabant & Gavaud (1985) have mapped their large extent in northern Cameroon. Two main types of these hard soils were distinguished (Lamotte, 1995): (i) massive, dense and hard clayey Vertisols that degrade structurally after cultivation (Brabant, 1987; Seiny-Boukar *et al.*, 1992), (ii) sandy (or sandy-loam) soils with a massive, dense and hard horizon, underlying less dense and looser horizons. For both types of soil, the hardness observed in the dry state disappeared when the samples were immersed in water. Hard soils were recognized as Solonetz (Bocquier, 1971), although Guis (1976) and Barbery & Gavaud (1980) pointed out that they lack the chemical characteristics of the natric horizon. Several authors suggested that sandy hard soils are derived from Planosols after an increase in translocation of clay (Gavaud *et al.*, 1976; Guis, 1976). However, one can see in the field two distinct layers, one with a dense and hard layer abruptly underlying a less dense and loose layer, which is not systematically associated with a wide variation in clay content nor with a perched water table. Thus, hard horizons in the Chad basin, of northern Cameroon particularly, were often considered either as 'sodium-pans' (within Solonetz) or as 'clay-pans' (within Planosols).

A massive, dense and brittle horizon that is strong when dry but which slakes when immersed in water is termed a fragipan. This term was introduced in the Soil Survey Manual (Soil Survey Division Staff, 1993), and there is an extensive literature describing and discussing fragipans (e.g. Smeck & Ciolkosz, 1989; Payton, 1992, 1993*a*,*b*; Bruckert & Bekkary, 1992). The origin of fragipans has been often related (i) to glacial or periglacial climates during the Quaternary in the northern hemisphere which induced an increase in bulk density under the weight of the ice, and (ii) to alternate shrinking and swelling with infilling of voids in glacial till (Miller *et al.*, 1971*a*,*b*). This explains why hard horizons in the subhumid and semi-arid tropics were rarely identified as fragipans. Nevertheless, other conditions were also evoked to explain the fragipan's differentiation, such as an alternating moist and dry climate which may induce the concentration of mineralogical binding agents between the skeleton grains (Franzmeier *et al.*, 1989), or as arid conditions which caused self-weight collapsing of a wetted sediment and then wetting and drying repeated cycles which induced physical ripening (Bryant, 1989). Thus, there is no unifying theory explaining the formation of fragipans, and several modes of soil differentiation could give to the physical characteristics like those recognized as specific in fragipans.

We have studied the characteristics of the hard horizon in a sandy-loam soil of the southern plain of the Chad basin. The fabric and porosity of the hard horizon are compared with the characteristics of the overlying loose horizon. A companion paper (Part II) by Lamotte *et al.* (1997) reports on the mineralogy of fine material involved in the hardening of the same soil.

The site

The site (*hardé Lagadgé*) is in northern Cameroon (10°25′N, 14°43′E), 50 km south-east of Maroua and approximately 200 km south of N'djamena (Fig. 1) in the southern plain of the Chad basin (Brabant & Gavaud, 1985). This plain has a regional slope of 1‰. The mean annual precipitation is 810 mm, and rain falls from May to September. The mean annual air temperature is 28°C, and the mean annual potential evapotranspiration is 1980 mm (data from Salak airport).

The landscape (Fig. 1) consists mainly of different types of vegetated land which alternate with bare ground (Lamotte, 1995): (i) shrubland where *Guiera senegalensis* and *Hexalobus monopetalus* are abundant with many other species of herbs and trees, (ii) grassland with *Aristida kerstingii, Indigofera nummularifolia, Loudetia togoensis* and *Zornia glochidiata* herbs species and locally the trees *Asparagus flagellaris, Balanites aegyptiaca, Cissus cornifolia, Guiera senegalensis* and *Lannea humilis*, (iii) bare ground with scattered herbs (*Schoenefeldia gracilis* and *Sporobolus festivus*) and trees (*Asparagus flagellaris, Balanites aegyptiaca* and *Lannea humilis*), and (iv) marsh with its characteristic vegetation. The topography is flat, except for the occurrence of erosion steps between bare ground and grassland.

The soil

The soil was studied along a NW–SE cross-section (Figs 1 and 2). Two sediments formed the parent materials (Fig. 2): (i) a heterogeneous alluvial material (from heavy clay to coarse sand) originating from Precambrian granito-gneiss of the Kaélé pediment, and (ii) an overlying homogeneous and continuous aeolian sandy-loam material originating from the Sahara desert.

The soil is developed mainly in the homogeneous sandy-loam sediment. According to the FAO legend of the world soil map (FAO–UNESCO, 1975), there are albic Arenosols in the shrubland, solodic Planosols in grassland, orthic Solonetz where the land is bare, and pellic Vertisols in the marsh. Detailed survey at the site showed a continuous, massive and hard sandy-loam horizon, which is overlain by a loose sandy-loam horizon of variable thickness (Fig. 2). The limit between the loose and the hard horizons is abrupt. The loose horizon is only a few centimetres thick in the bare zones and about 20–40 cm in the grassland. Where there are trees the hard horizon either occurs deeper than 4 m from the surface or is absent (Lamotte *et al.*, 1994). Table 1 gives a description of the typical sandy-loam soil from the shrubland and grassland.

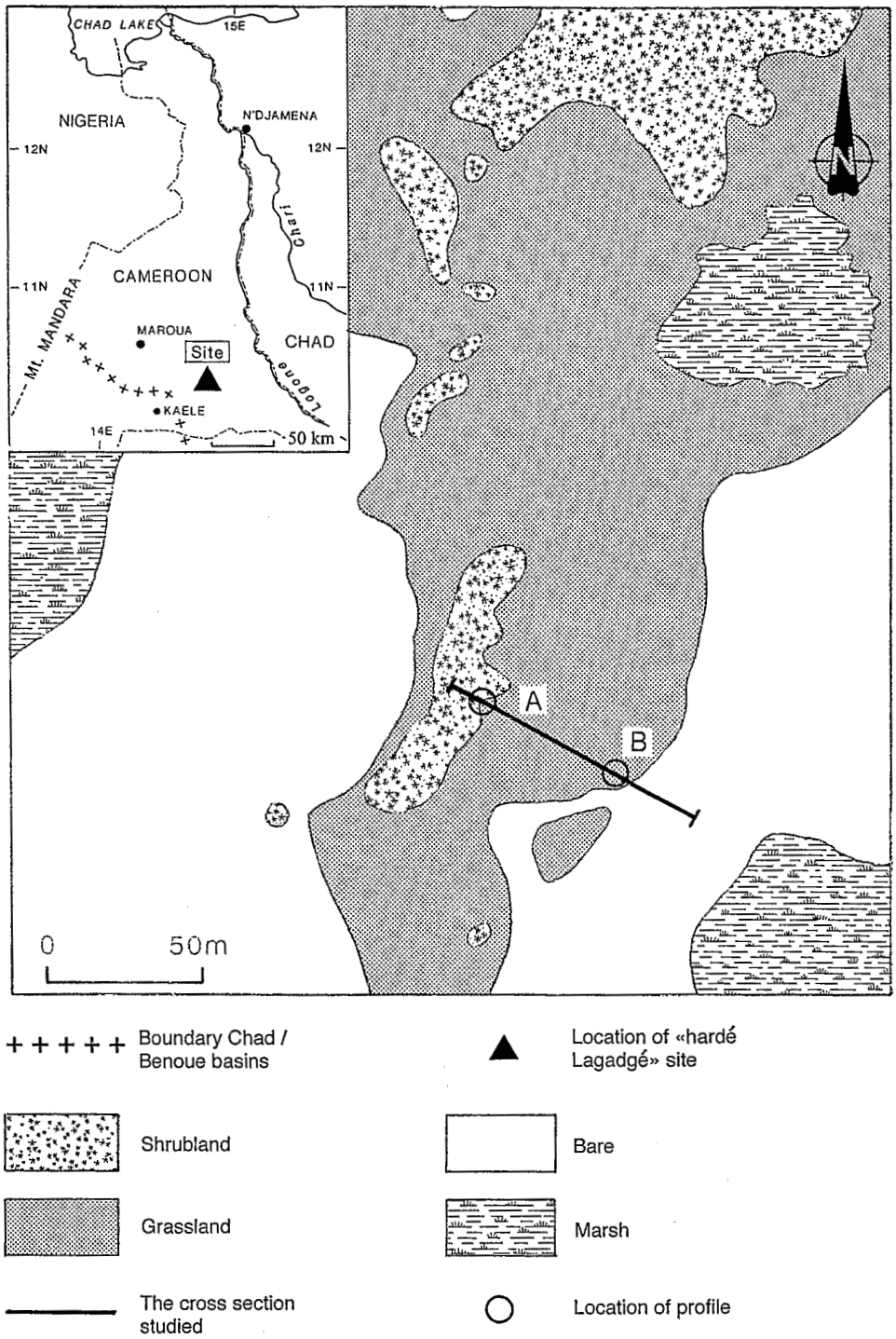

Fig. 1 Location of study site (*hardé Lagadgé*) in northern Cameroon and detailed landscape map showing the extent of shrubland, grassland, bare ground and marsh with their characteristic vegetation.

Field sampling

Two profiles of sandy-loam soil with an abrupt transition between the loose and hard horizons were selected (Figs 1 and 2). Profile A was at the contact between shrubland and grasslands and corresponded to the limit between albic Arenosols and solodic Planosols (Fig. 2). Profile B was a solodic Planosol. For the two profiles, if we consider the rupture resistance as defined in the Soil Manual Survey (Soil Survey Division Staff, 1993), the loose horizon was friable to

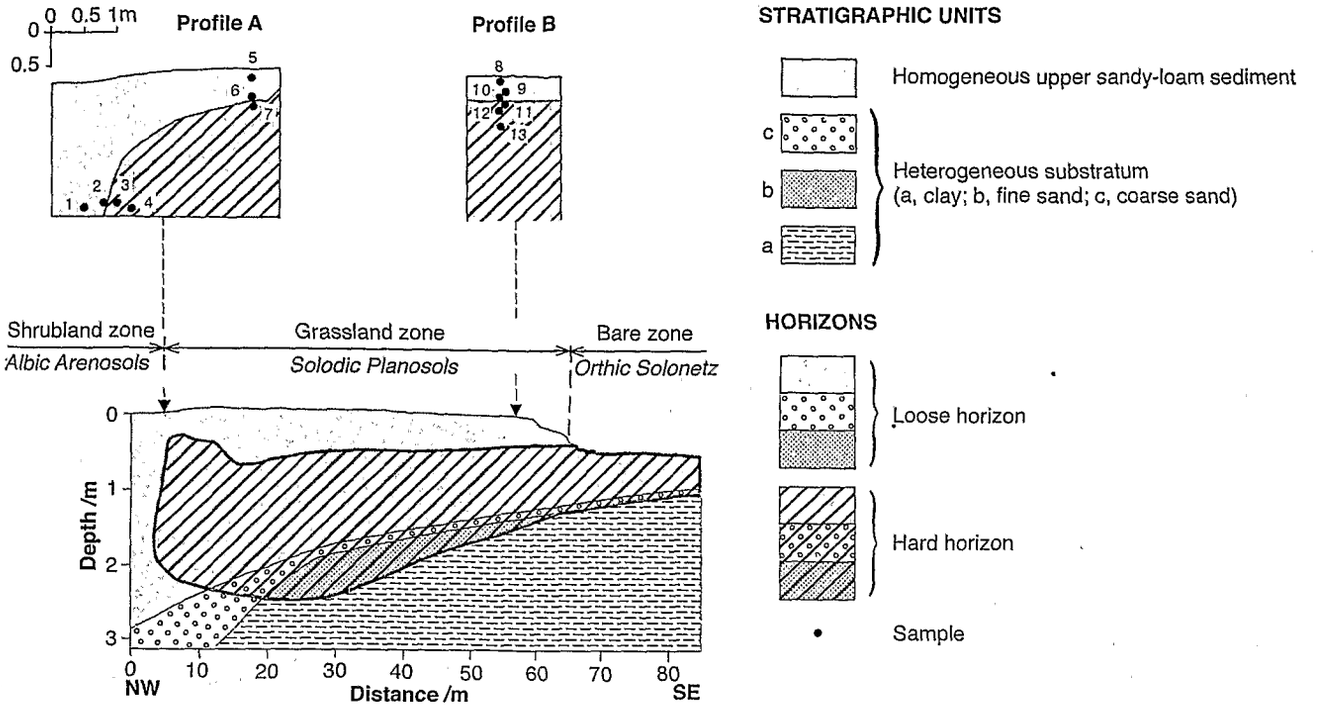

Fig. 2 Distribution of sediments and pedological horizons along the cross section shown in Fig. 1 (soil classification according to FAO–UNESCO, 1975).

Table 1 Selected morphological, physical and chemical properties of the typical soil developed in the shrubland (albic Arenosol) and grassland (solodic Planosol)

Soil (FAO)[a]	Albic Arenosol				Solodic Planosol					
Horizon (FAO)[a]	Au1	Au2	AE	E	AU	Au2	E	Btx1	Btx2	Btx3
Depth /cm	0–20	20–70	70–170	170–270	0–15	15–32	32–35	35–37	37–45	45–120
Munsell moist colour	10YR5/3	10YR5/6	10YR5/8	10YR7/3	10YR4/4	10YR6/4	10YR6/6	10YR5/3	10YR5/6	2.5Y5/4
Structure[b]	s g	s g	s g	s g	s g	s g	s g	m	m	m
Concretions[c]	—	—	f Fe	m Fe	—	—	—	—	—	f Fe-f Ca
Boundary[d]	grad	grad	grad	grad	grad	grad	abr	grad	grad	grad
Particle size /g 100 g^{-1}										
Clay (0–2 μm)	8	10	7	4	6	10	3	11	19	26
Silt (2–50 μm)	20	18	20	28	14	19	22	19	20	20
Fine sand (50–200 μm)	53	53	54	51	51	47	53	52	44	43
Coarse sand (> 200 μm)	19	19	19	17	29	24	22	18	17	11
Bulk density[e] /g cm^{-3}	1.6	1.5	1.6	1.6	ND	1.5	ND	1.9	1.9	1.8
Porosity[f] /cm^3 100 cm^{-3}	40	44	40	40	ND	44	ND	29	30	33
Exchangeable cations[g]										
CEC /cmol kg^{-1}	1.8	0.8	1.0	0.9	1.5	0.6	1.5	ND	4.7	9.9
Ca /cmol kg^{-1}	<0.1	<0.1	0.4	<0.1	0.3	0.4	0.4	ND	1.3	2.0
Mg /cmol kg^{-1}	<0.1	<0.1	<0.1	<0.1	<0.1	0.1	<0.1	ND	0.3	0.6
K /cmol kg^{-1}	<0.1	<0.1	<0.1	<0.1	0.1	0.1	0.1	ND	0.1	0.1
Na /cmol kg^{-1}	<0.1	<0.1	0.1	<0.1	<0.1	<0.1	0.3	ND	1.5	2.1
C Total[h] /g kg^{-1}	2.8	1.8	0.8	0.4	1.2	1.3	0.7	ND	1.2	0.8
ph (H_2O)[i]	4.4	3.6	4.2	4.5	4.3	5.2	5.7	ND	8.1	8.7

[a]According to FAO–Unesco (1975). [b]m, massive and s g, single grain structure. [c]f, few, m, many, Fe ferruginous concretions, Ca carbonate concretions. [d]grad, gradual and abr, abrupt. [e]Determined in triplicate on cores (100 cm^3). [f]Calculated from bulk density with particle density = 2.65 g cm^{-3}. [g]Measured by atomic absorption spectrophotometry after extraction with $BaCl_2$ and saturation by $MgSO_4$. [h]Determined by dry combustion with a CHN analyser. [i]Measured in 2.5:1 soil water slurries with distilled water.

very friable, whereas the hard horizon was very firm to extremely firm. The loose and hard horizons had a single grain and massive structure, respectively. The hard horizon was moderately brittle when it was wet and it slaked when immersed in water. In the profile A the limit between the loose and the hard horizons changed from being essentially horizontal in the SE to being essentially subvertical in the NW (Fig. 2). In the profile B, in another part of the grassland, the limit between the loose and the hard horizons was essentially horizontal. Disturbed and undisturbed samples were collected, particularly at a few centimetres on each side of the limit between the horizons. Collection of undisturbed samples from the hard horizon required a bell-shaped saw (4.5 cm in diameter and 6 cm deep) with diamond or tungsten carbide teeth.

Laboratory methods

Scanning electron microscopy

To describe the fabric of the loose and hard horizons we used a scanning electron microscope (SEM, Cambridge 90B) working in the secondary electron mode on small fragments and in the backscattered mode on thin sections.

The fragments (10 mm^3 in size) with natural breaking surfaces were mounted on 1.2-cm diameter aluminium stubs with silver paint and were coated with about 25 nm of gold in a sputter coater.

For thin section preparation, undisturbed and orientated blocks were oven-dried at 40°C for 1 week and impregnated under vacuum of 5 kPa with a polyester resin diluted with 30% (volume) of a styrene monomer (Bruand *et al.*, 1996). Thin sections (4.5 × 6 cm) were prepared following the method of Fitzpatrick (1984). They were polished with diamond grains of decreasing size (down to 0.25 μm), sprayed on polishing sheets, and the polished surface was coated with carbon. The examination of polished surface in scanning electron microscopy using the backscattered electrons enabled us to distinguish the voids occupied by the resin, which appear black, from the soil mineral constituents which appear lighter with a resolution of about 0.1 μm (Kooistra & Tovey, 1994). Image analyses were made with VISILOG software. Nine pictures (0.5 × 1 mm), obtained at magnification of ×50, were selected for each of the loose and hard horizons. The total surface area of the pictures was represented by about 400 × 103 pixels. These pictures enabled us to calculate the surface area occupied by skeleton grains in each type of horizon.

Particle size distribution

After treatment with H_2O_2 to remove organic matter, the soil samples (30 g) were shaken for 16 h with 300 ml of distilled water. Particles with diameter larger than 50 μm were collected by sieving. The size distribution for particles with diameter ranging from 50 to 2500 μm was determined by sieving (after treatment with HCl to remove ferruginous concretions). For the finer particles (50–0.2 μm), the size distribution was obtained using a 5000 ET Sedigraph (Singer *et al.*, 1988). The particles size distribution (psd) curve was derived from the cumulative frequency curve for diameter exceeding 2 μm, and each point of the psd curve represents the slope of the cumulative curve between two successive values of diameter.

Mercury porosimetry

The cumulative void volume (cvv) curve was determined with a mercury porosimeter measuring both the pressure required to force mercury into the voids of a dry sample and the volume of intruded mercury at each pressure. If we assume that the voids are cylindrical then the relation between equivalent void diameter (D expressed in μm) and applied pressure (P expressed in Pa) is:

$$D = -4\sigma(\cos\theta)/P,$$

where σ is the surface tension of mercury and θ its contact angle on the soil material. The values of σ and θ were taken as 0.484 N m^{-1} and 130° respectively. Mercury porosimetry was done with a Micromeritics 9310 porosimeter operating to a maximum pressure of 200 MPa (Fiès, 1984). Thus, the cvv was measured for voids between 0.006 and 370 μm equivalent cylindrical diameter. Measurements were made on three replicate undisturbed fragments of 0.5–1 cm^3, dried at 105°C for 24 h. All the volumes of mercury intruded between 40 and 200 MPa were corrected for mercury compression. The volume of voids was expressed on a mass basis (mm^3 g^{-1}). The cvv curve and its first-derivative, i.e. the void size distribution (vsd) curve, were used to discuss the results (Bruand & Prost, 1987).

Results

SEM observations

The observation of thin-sections (Fig. 3a, c) obtained for the loose and the hard horizons showed that skeleton grains ranged from fine silt (≈ 10 μm in diameter) to coarse sand (≈ 300 μm). The skeleton grains were well-sorted with variable shapes with sharp or rounded corners (angular or subangular grains). Image analysis on thin sections showed that the surface area occupied by the skeleton grains (Fig. 3b, d) was 53.4% in the loose horizon and 53.1% in the hard horizon with standard deviations of 4.1 and 2.1, respectively.

The loose horizon contained only a small proportion of clay in the groundmass. The skeleton grains were generally uncoated and not linked to adjacent grains (Figs 3a and 4a, b). Thin-sections showed also that the voids consisted mainly of

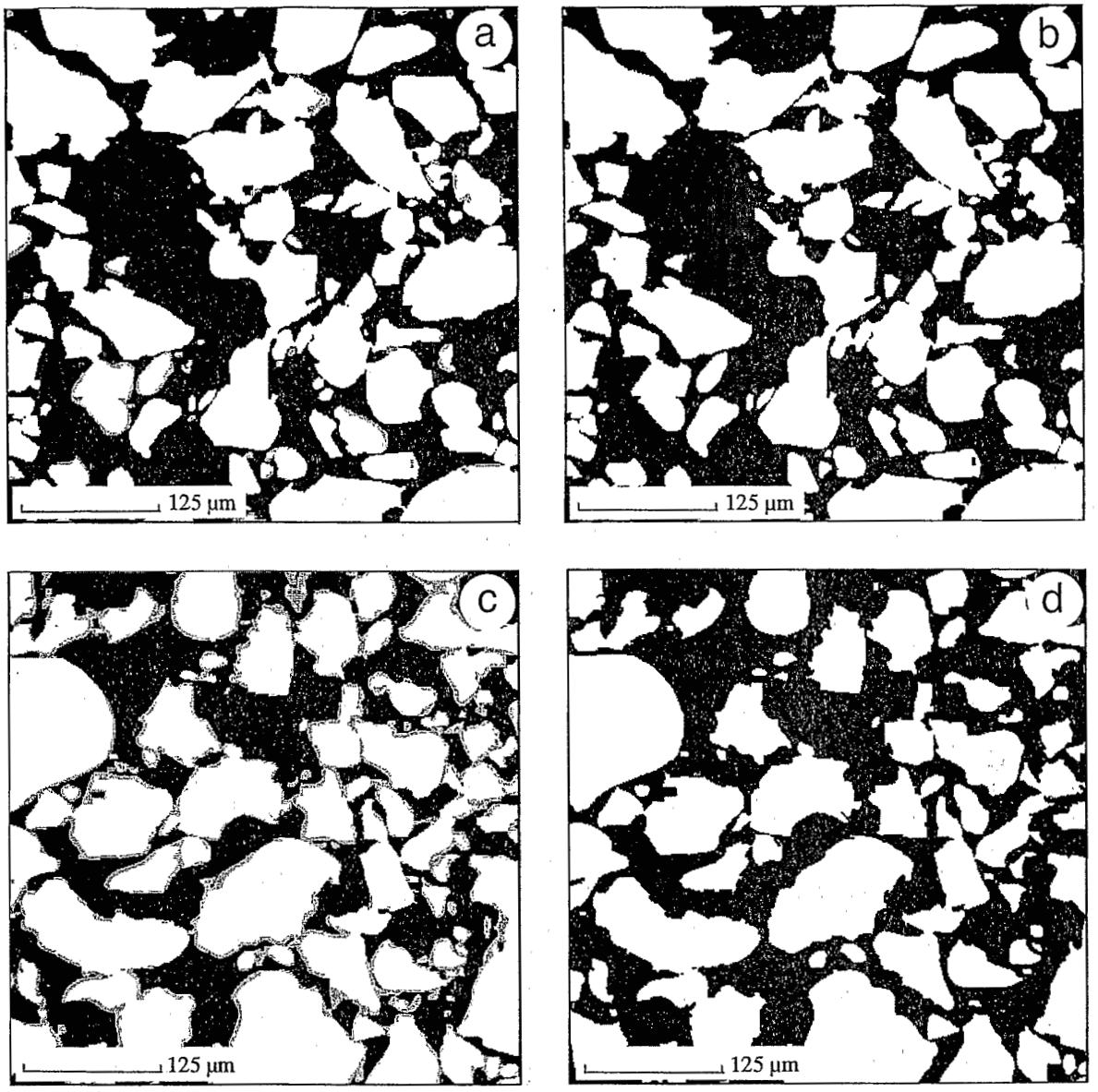

Fig. 3 Backscattered-electron image obtained from thin section: (a) from the loose horizon, (c) from the hard horizon (black areas are pores, white areas are skeleton silt or sand grains, and heterogeneous grey areas are clay particles with associated pores forming the coatings on skeleton grains or the linkages between them); (b) and (d) pictures showing the corresponding areas occupied by skeleton grains.

packing voids between skeleton grains (from 20 to 200 µm) and secondarily of vughs (200–1000 µm). The voids were of irregular shape and were well-interconnected (Fig. 3a).

In the hard horizon the skeleton grains were covered by clay coatings and linked by clay bridges (Fig. 3c). The latter were wall-shaped and their thickness varied with their length: 10–40 µm long and 0.5–1 µm thick for the longest, and 5–10 µm long and 15–30 µm thick for the shortest (Fig. 4c to g). Coatings on the surface of the skeleton grains were 0.5–10 µm thick. Both coatings and wall-shaped linkages were made of a fine material dominated by very small clay particles (difficult to identify individually by SEM) including a few small grains (0.5–3 µm). The wall-shaped linkages were firmly anchored to the skeleton grains because of the continuity of the fine material between them and the coatings on the skeleton grain surfaces. The fabric of coated skeleton grains with wall-shaped linkages showed a continuous design without any preferential orientation in the groundmass. This horizon appeared less porous in thin-section than the loose horizon (Fig. 3a and b). The voids were smaller than in the loose horizon because they were partly filled by the fine material mentioned above. Packing voids ranged from 10 to 150 µm in size and vughs from 50 to 700 µm. All the voids were rounded and they were either weakly interconnected or closed.

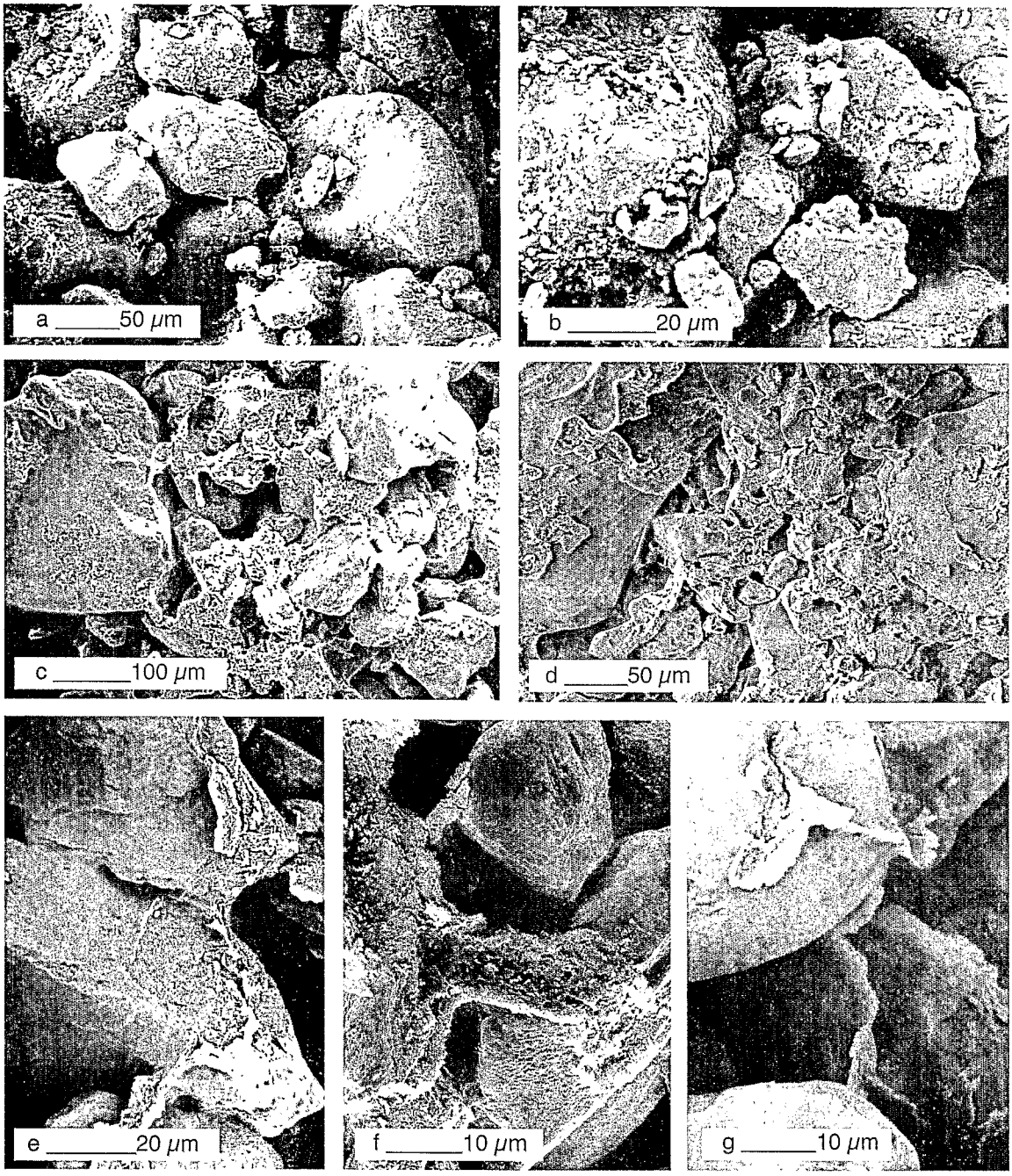

Fig. 4 SEM micrographs (secondary electron mode) of broken surfaces of small fragments: (a) and (b) fabric of the loose horizon with well-interconnected packing voids between silty and sandy skeleton grains (free from coatings and linkages); (c) and (d) fabric of the hard horizon showing closed or weakly interconnected voids between skeleton grains coated by clay and bounded by clay wall-shaped bridges; (e), (f) and (g) intergranular voids showing the continuity of the clay from the wall-shaped bridges to the coatings on the skeleton grain surfaces and main morphological variety of wall-shaped bridges.

Particle size distribution

All the samples (Fig. 2) exhibited two populations of particles (Table 2 and Fig. 5): (i) particles belonging to both fine sand (50–500 μm) and coarse silt (20–50 μm) fractions, and (ii) particles belonging to the clay fraction (<2 μm). The sum of sand and silt ranged from 89.8 to 97.4% in the loose horizon and from 68.4 to 93.6% in the hard one.

Cumulative frequency curves of the particles greater than 2 μm were sigmoidal, as illustrated for the samples 8–13

Table 2 Particle size distribution for samples from the loose and the hard horizons. Relative percentage frequency by standard fractions and characteristics of particle size distribution curves for particles > 2 μm

	Profile A							Profile B					
Horizon[a]	L		H		L		H	L			H		
Sample[b]	1	2	3	4	5	6	7	8	9	10	11	12	13
Depth /cm	187	185	180	205	12	47	53	7	22	34	36	42	75
Relative percentage frequency by standard fractions for the fine particles (<2 μm) and coarse particles (≥2 μm) /g 100 g^{-1}													
<0.2 μm	0.6	0.3	1.6	23.9	3.4	1.0	10.2	3.2	4.2	1.0	7.3	14.1	12.8
0.2–2 μm	3.7	2.3	4.8	7.0	4.4	3.1	55.0	3.0	6.0	1.9	3.4	5.1	13.1
Total <2 μm	4.3	2.6	6.4	30.9	7.8	4.1	15.7	6.2	10.2	2.9	10.7	19.2	25.9
2–20 μm	16.0	15.6	17.1	9.0	8.2	10.3	9.3	4.6	7.5	6.5	5.8	7.7	9.2
20–50 μm	12.4	22.1	20.5	14.2	14.5	13.3	14.6	9.8	11.7	15.6	13.2	11.8	11.1
50–100 μm	27.0	31.0	29.7	22.9	26.9	26.6	23.0	23.7	22.8	26.9	26.8	22.0	22.2
100–200 μm	23.6	19.3	16.6	14.7	24.8	26.6	20.3	27.0	24.4	26.2	25.6	22.1	20.4
200–500 μm	11.6	7.2	6.9	5.7	12.9	14.1	10.5	18.4	14.8	13.7	11.7	10.8	8.2
500–1000 μm	3.6	2.2	2.8	1.9	4.9	5.0	4.5	8.7	6.6	5.3	4.2	4.0	1.9
1000–2000 μm	1.5	—	—	0.7	—	—	2.1	1.6	2.0	2.9	2.0	2.0	1.1
> 2000 μm	—	—	—	—	—	—	—	—	—	—	—	0.4	—
Total > 2 μm	95.7	97.4	93.6	69.1	92.2	95.9	84.3	93.8	89.8	97.1	89.3	80.8	74.1
Characteristics of the size distribution for coarse particles (> 2 μm)													
Median /μm[c]	85	65	62	70	95	95	85	108	102	95	95	95	85
Inter-Quartile slope[c]	102	97	92	114	105	105	94	94	88	93	115	105	113
Maximum /μm[d]	100	80	80	85	95	100	95	105	105	100	100	100	100

[a]L, loose and H, hard. [b]See Fig. 2 for the location of the samples. [c]Characteristic of the cumulative curve. [d]Characteristic of the derivative curve.

(Fig. 6a). The median and interquartile slope values were similar for all the samples (Table 2). The psd curves for the samples 8–13 were unimodal with a well-defined maximum (Fig. 6b). For all the samples, this maximum varied weakly between 80 and 105 μm (Table 2).

Clay content ranged from 2.6 to 10.2% in the loose horizon and from 6.4 to 30.9% in the hard one (Table 2). The content of fine clay (<0.2 μm) ranged from 0.6 to 4.2% and from 1.6 to 23.9% in the loose and hard horizons, respectively. The clay content and the proportion of fine clay increased with depth (samples from 11 to 13) and laterally (samples 3 and 4) within the hard horizon whereas there was no regular variation within the loose one (Table 2).

Void size distribution

Cumulative mercury intrusion curves showed a wide variation in the total volume of intruded mercury (V_{Hg}) between the loose horizon (V_{Hg} 295 mm^3 g^{-1}) and the hard one (157 ⩽ V_{Hg} ⩽ 191 mm^3 g^{-1}). Thus, V_{Hg} was about 110 mm^3 g^{-1} smaller for samples from the hard horizon than for those from the loose horizon (Fig. 7a and Table 3).

The derivative of the cumulative curves indicated that the total pore volume V_{Hg} consists of two distinct pore volumes (coarse voids, C; fine voids, F) for samples from the loose and the hard horizons (Fig. 7b). Each void volume is defined by its volume per unit mass of solid (V) and by its modal diameter (D_m) which corresponds to maximum of the void size distribution (vsd) curve. The values are listed in Table 3. D_m ranged from 3 to 30 μm for the main mercury entry 0.1 < D < 300 μm (coarse void volume V_C). This first mercury entry is followed by a second one which occurred for diameter D < 0.1 μm with D_m ⩽ 0.01 μm (fine void volume V_F). The vsd curves obtained for the loose horizon showed that V_C

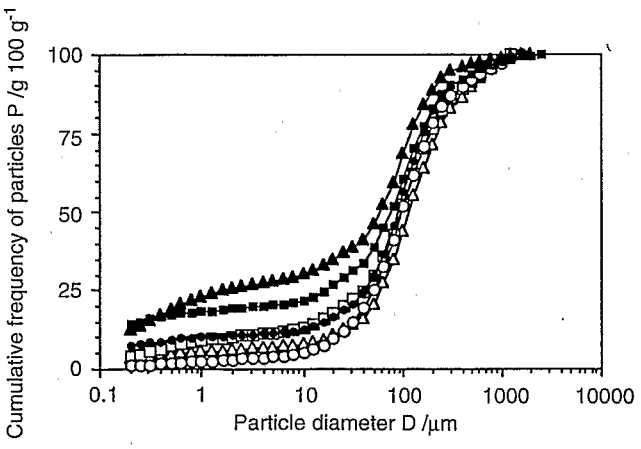

Fig. 5 Cumulative frequency diagrams of the particles >0.2 μm for samples from the loose horizon (samples 8, △; 9, □; 10, ○) and from the hard horizon (samples 11, ●; 12, ■; 13, ▲).

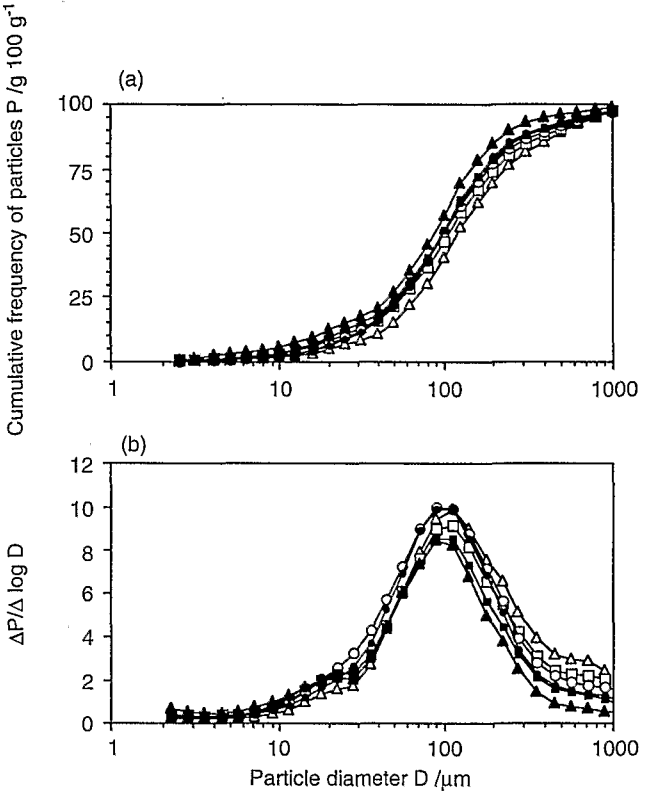

Fig. 6 (a) Cumulative frequency curve and (b) particle size distribution (psd) curve of skeletal particles > 2 μm for samples from the loose (samples 8, △; 9, □; 10, ○) and from the hard horizon (samples 11, ●; 12, ■; 13, ▲).

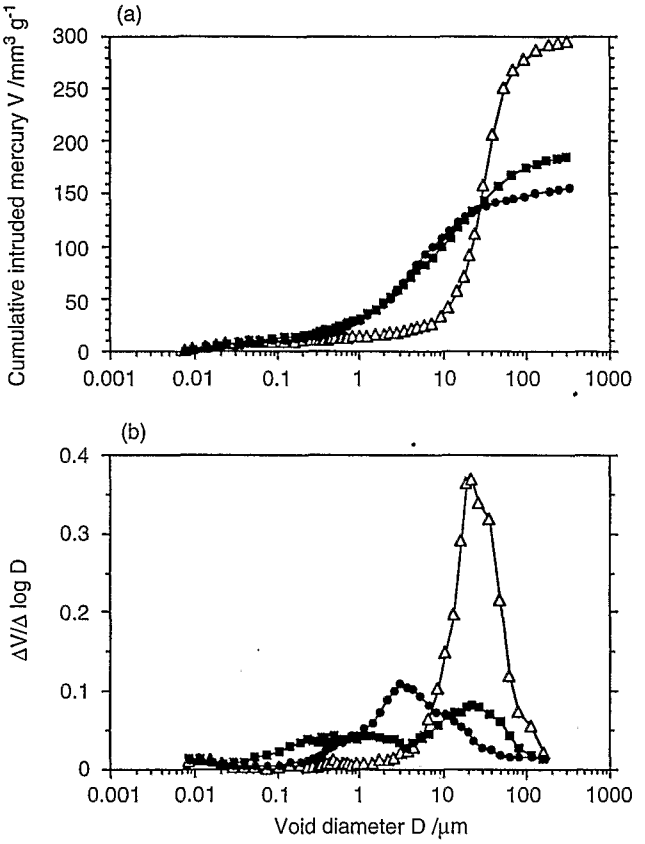

Fig. 7 (a) Cumulative mercury intrusion and (b) void size distribution (vsd) curves obtained for the loose horizon (sample 8, △) and for the hard horizon (samples 11, ●; 12, ■; 13, ▲).

ranged from 287 to 293 mm^3 g^{-1} (97–99% of V_{Hg}) whereas it ranged from 147 to 182 mm^3 g^{-1} (94–96% of V_{Hg}) in the hard horizon (Table 3).

Discussion and conclusion

Origin of hardness

Particle size distribution showed the granulometric homogeneity of particles > 2 μm (fine sandy loam) in both the loose and the hard horizons. Moreover, where small differences were observed, they are not related to the consistency. Rather, they are probably due to variation in the sedimentary conditions. This lithological homogeneity of the material is consistent with the results from Lamotte (1995) who showed that skeleton grains in the loose and hard horizons are composed mainly of quartz (⩾95%), weathered K-feldspars (⩽4%), with the same heavy mineral suite (⩽1%). A similar lithological homogeneity was earlier demonstrated for the loose and hard horizons of Planosols and Solonetz in Chad (Bocquier, 1971).

The hard horizon cannot be distinguished easily from the loose horizon on the basis of clay content, as similar clay contents were observed for samples from both. The cumulative frequency curves (Fig. 5) showed that the variation in the clay content occurs mainly in the fine clay fraction (Table 2). The increase in the fine clay content can be small and it can occur over 1–2 cm from each side of the limit separating the loose and the hard horizons. Indeed, this increase was 1.3% between the samples 2 and 3 originating from the hard and the loose horizons, respectively (Fig. 2 and Table 2).

Scanning electron micrography showed that the hardness is closely related to the presence of both clay coatings on the skeleton grains and clay wall-shaped bridges linking them. The groundmass fabric of the skeleton grains with clay coatings and clay bridges is specific to the hard horizon for a large range of clay contents, thus demonstrating that loose and hard horizons may have a similar clay content. Nevertheless, the common presence of coatings on skeleton grains and wall-shaped bridges requires a minimum clay content. It can be roughly estimated as about 6%, i.e. the smallest clay content measured in the hard horizon. Thus the increase in the proportion of fine clay in the hard horizon is consistent with the SEM observations, showing that the coatings and bridges consist mainly of very fine clay particles. The SEM showed also the continuity of the fine material from the coatings to the

Table 3 Total volume of mercury intruded (V_{Hg}), characteristics of elementary void volumes C and F (modal diameter D_m and void volumes V_C and V_F) and total porosity (P) obtained by mercury intrusion for samples from loose and hard horizons

	Profile A						Profile B								
Horizon[a]	L			H			L			H					
Sample[b]	6			7			8			11			12		
Depth/cm	47			53			7			36			42		
	m[c]	min	max	m	min	max	m	min	max	m	min	max	m	min	max
V_{Hg}/mm^3 g^{-1}	295	278	318	191	184	196	296	269	324	157	151	161	184	160	213
Void volume C															
D_m/μm	23	23	49	11	11	17	26	23	36	4	3	4	17	5	23
V_C/mm^3 g^{-1}	293	277	312	182	175	188	287	267	304	147	140	152	173	151	203
$(V_C/V_{Hg}) \times 100$	99	98	100	95	94	97	97	94	99	94	93	94	94	93	95
Void volume F															
V_F/mm^3 g^{-1}	2	0	6	9	6	11	9	2	20	10	9	11	11	9	12
$(V_F/V_{Hg}) \times 100$	1	0	2	5	3	6	3	1	6	6	6	7	6	5	7
Porosity P/‰	44	42	46	33	33	34	44	42	46	29	29	30	33	30	36

[a]L, loose and H, hard. [b]See Fig. 2 for the location of the samples. [c]m, Mean (mean curve obtained with three replicate analysis), minimum and maximum between replicate analysis.

bridges and from the longest to the shortest wall-shaped bridges. The examination of the wall-shaped bridges from different angles of view showed that the thickness generally decreases from the skeleton grain contact to the intergranular void centre. Thus, a large morphological variety of wall-shaped bridges corresponding to different fracture surfaces of the same type of object can be observed (Fig. 8).

Our results indicate that the hardness of sudano-sahelian soils containing little clay is closely related to a specific fabric, where the skeleton grains are coated and linked by wall-shaped

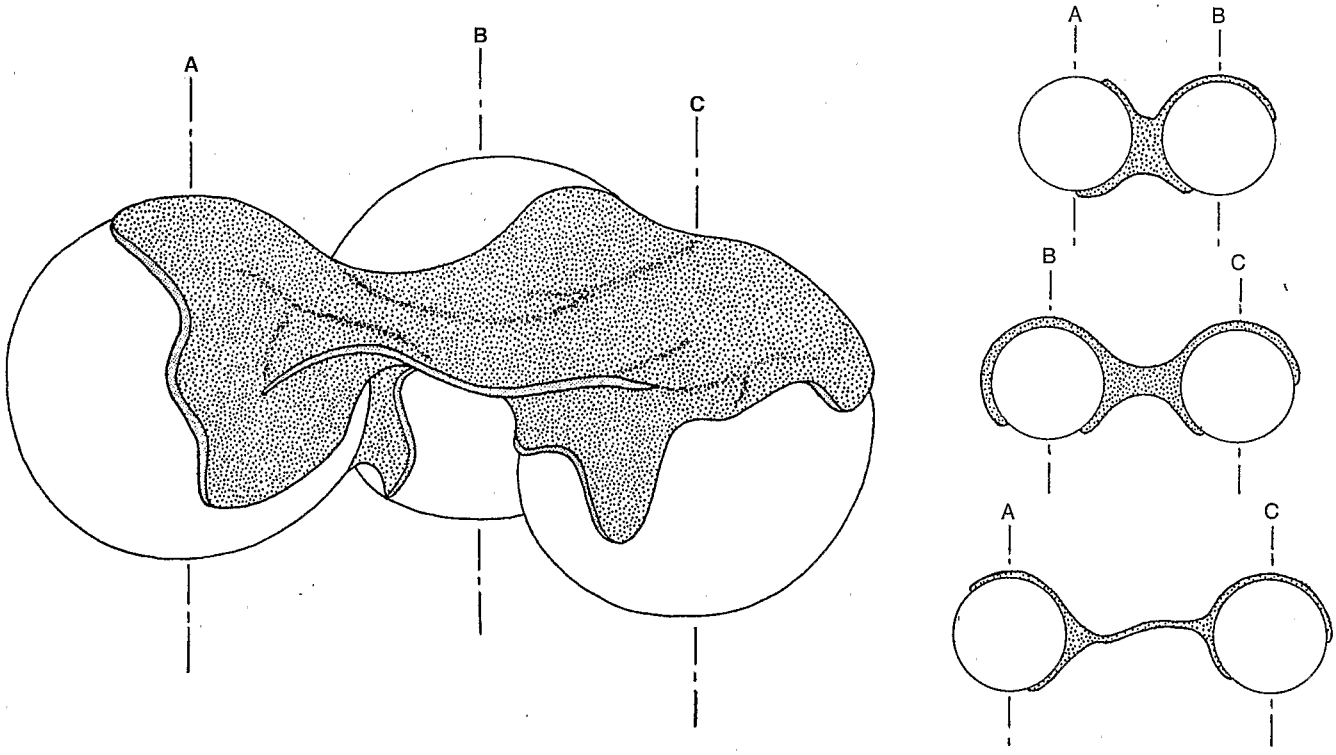

Fig. 8 Schematic representation of the groundmass fabric showing the variety in morphologies of wall-shaped bridge observed on thin section.

bridges made of fine clay particles. The genesis of this fabric would be favoured by the development of perched ground water with abundant fine clay in suspension (minerals inherited or formed *in situ*). The formation of wall-shaped bridges could be caused by the evaporation of the perched ground water, as suggested by their meniscus morphology.

Comparison with fragipans

Clay coating the skeleton grains and clay wall-shaped bridges linking the latter were also observed for fragipans samples using microscopy (McKeague & Wang. 1980; Bridges & Bull, 1983).

Earlier studies have also shown little or no difference in the size distribution of the skeleton grains (Lozet & Herbillon, 1971; Payton, 1992) or in the total clay content (Bridges & Bull, 1983) between a fragipan and its overlying horizon. The increase in the fine clay content which was recorded between the loose and the hard horizons was observed in fragipan relative to overlying horizons (Jamagne *et al.*, 1984; Payton, 1992).

The development of clay coatings and clay bridges causes a sharp decrease in the porosity since V_{Hg} was about 30% less in the hard horizon than in the loose one. This was consistent with the increase in bulk density which was revealed with core samples of 100 cm^3 (Table 1). Taking the particle density as 2.65 g cm^{-3}, the calculated porosity ranges from about 40–44% and from about 29–33% in the loose and hard horizons, respectively. Less porosity in fragipans relative to the overlying horizons was observed in several soil profiles (DeKimpe *et al.*, 1972; Payton, 1992). Nevertheless, it is now recognized that fragipan differentiation is not systematically associated with an increase in bulk density (Lindbo *et al.*, 1994).

Mercury porosimetry showed that the volume of fine voids V_F is not significantly different between the loose and hard horizons. Thus, the decrease in the total porosity is related mainly to a decrease in the volume of coarse voids V_C (about 100 mm^3 g^{-1}) associated with a decrease in the corresponding modal diameter (23–24 μm in the loose horizon and 3–14 μm in the hard one). Similar results were obtained in fragipans from Belgian soils (Lozet & Herbillon, 1971), from several USA soils (Olson, 1985) and from Italian soils (Ajmone-Marsan *et al.*, 1994).

We interpreted V_C and V_F as the volume of pores resulting from the fabric of skeleton grains with the clay phase and from the packing of clay particles within the clay phase, respectively, as discussed earlier by Bruand & Cousin (1995). Because the clay particles are so small, their associated packing porosity was investigated in part by mercury porosimetry (Bruand & Prost, 1987). Thus, the value of V_F cannot be closely related to clay content. Furthermore, the large decrease in V_C and in its modal diameter can be related to the increase of the volume of the clay phase and its associated porosity. This is consistent with SEM observations.

For the fragipans from Belgian soils, Lozet & Herbillon (1971) concluded that the decrease in porosity resulted from compression during periglacial periods. Here, image analysis (Fig. 3c, d) indicated that the proportion of area occupied by the skeleton grains was similar at the bottom of the loose and at the top of the hard horizon (53.4 and 53.1%, respectively). Thus, no difference in the packing of the skeleton grains was observed between the two types of horizon. The decrease of the porosity in the hard horizon is related to the presence of clay coatings around skeleton grains and wall-shaped clay bridges between them.

Hence, the hard horizon has a particle size distribution and a fabric displaying many similarities with fragipans described elsewhere. It has the consistency of fragipans when dry and slakes when immersed in water. Nevertheless, the brittleness of the hard horizon when it is wet is not as well as developed as in horizons recognized as fragipans. The similarities between the characteristics of the hard horizon and those described earlier for fragipans would indicate similarities in their origin. Some authors suggest that the origin might be related to a periglacial climate (Miller *et al.*, 1971*a*, *b*), others think it would be arise in an alternate moist and dry climate (Franzmeier *et al.*, 1989). Actually, alternate dry and moist conditions would be required for the formation of the groundmass fabric of the hard horizons and fragipans. Indeed, freezing is equivalent to a strong drying for the fabric of the groundmass, as water moves from the pores of the groundmass to macropores where ice crystals grow. Hence, periglacial climate in the northern hemisphere and semi-arid and arid climate in the tropics induce a strong drying of the soil which would be responsible for the close fabric of the groundmass.

Consequences of the groudmass fabric

The poor development of macrostructure, with only large prisms (0.5 m in size), would result from the properties of the fabric. Clay shrinkage and swelling would be balanced by an increase and loss in the porosity between the skeleton grains, thus impeding the development of a macroscopic crack network. Conversely, the small permeability of the hard horizon would also limit water movement and consequently shrink–swell phenomena. Thus, the continuity of the solid phase in the groundmass of the hard horizon and the lack of macroscopic structure explain the considerable strength of this horizon, and consequently the difficulties for root penetration and tillage. Consequently, the trees grow mainly where the hard horizon is absent, and the distribution of shrubland and grassland is closely related to the presence and depth of the hard horizon.

Finally, our results also explain the difficulty in generating a structure to restore physical properties of the soils with a hard horizon. Indeed, hardness might result from characteristics of the fabric at a microscopic scale, and these features cannot be easily changed. Biological activity can introduce disorder and

porosity in the regular design of the fabric, but the very small humectation of the hard horizon in the rainy season is not in favour of this activity. Other studies should be carried out to explain the differentiation of hard horizons as a function of their fabric. The management of the sandy and sandy-loam soils should attempt to avoid overdrying the horizons with this kind of fabric.

Acknowledgements

We thank M. Delaune (Institut Français de la Recherche Scientifique pour le Développement en Coopération, Bondy) for granulometric measurements and helpful discussions, and S. Desbourdes, C. le Lay and L. Rousset (Institut National de la Recherche Agronomique, Orléans) for technical assistance.

References

Ajmone-Marsan, F., Pagliai, M. & Pini, R. 1994. Identification and properties of fragipan soils in the Piemonte region of Italy. *Soil Science Society of America Journal,* **58,** 891–900.

Barbery, J. & Gavaud, M. 1980. Notice de la carte. In: *Carte pédologique du Nord-Cameroun à 1/100 000. Feuille Bogo-Pouss.* ORSTOM and ONAREST–IRAF, Paris.

Bocquier, G. 1971. Genèse et évolution de deux toposéquences de sols tropicaux du Tchad. Interprétation biogéodynamique. *Cahiers de l'ORSTOM. Série Pédologie,* **9,** 509–515.

Brabant, P. 1987. Management of vertisols under semi-arid conditions. In: *Selection of Sites for the Vertisols Network: Distinction between Types of Vertisols* (eds M. Latham, P. Ahn and C.R. Elliot), pp. 65–70. IBSRAM Proceedings, Bangkok.

Brabant, P. & Gavaud, M. 1985. Contraintes et aptitudes des terres. In: *Les sols et les ressources en terres du Nord-Cameroun.* ORSTOM and ONAREST, Paris.

Bridges, E.M. & Bull, P.A. 1983. The role of silica in the formation of compact and indurated horizons in the soils of South Wales. In: *Soil Micromorphology, Proceedings of the 6th International Working Meeting on Soil Micromorphology* (eds P. Bullock and C.P. Murphy), pp. 605–613. A.B. Academic Publishers, Berkhamsted, UK.

Bruand, A. & Cousin, I. 1995. Variation of textural porosity of a clay-loam soil during compaction. *European Journal of Soil Science,* **46,** 377–385.

Bruand, A. & Prost, R. 1987. Effect of water content on the fabric of a soil material: An experimental approach. *Journal of Soil Science,* **38,** 461–472.

Bruand, A., Cousin, I., Nicoullaud, B., Duval, O. & Bégon, J.C. 1996. Backscattered electron scanning images of soil porosity for analyzing soil compaction around roots. *Soil Science Society of America Journal,* **60,** 895–901.

Bruckert, S. & Bekkary, M. 1992. Formation des horizons diagnostiques argiliques et de fragipan en fonction de la perméabilité des roches. *Canadian Journal of Soil Science,* **72,** 69–88.

Bryant, R.B. 1989. Physical processes of fragipan formation. In: *Fragipans: Their Occurrence, Classification and Genesis* (eds N.E. Smeck and E.J. Ciolkosz), pp. 141–150. Soil Science Society of America, Special Publication No. 24, Madison, WI.

DeKimpe, C.R., Baril, R.W. & Rivard, R. 1972. Characterization of a toposequence with fragipan. The Leeds-Ste. Marie-Brompton series of soils. Province of Quebec. *Canadian Journal of Soil Science,* **52,** 135–150.

FAO–UNESCO. 1975. *Soil Map of the World (1/5 000 000).* FAO, Paris.

Fiès, J.C. 1984. Analyse de la répartition du volume des pores dans les assemblages argile-squelettes. Comparaison entre un modèle d'espace poral textural et les données fournies par la porosimétrie au mercure. *Agronomie,* **4,** 891–899.

Fitzpatrick, E.A. 1984. *Micromorphology of Soils.* Chapman & Hall, London.

Franzmeier, D.P., Norton, L.D. & Steinhardt, G.C. 1989. Fragipan formation in loess of the midwestern United States. In: *Fragipans: Their Occurrence, Classification and Genesis* (eds N.E. Smeck and E.J. Ciolkosz), pp. 69–97. Soil Science Society of America, Special Publication No 24, Madison, WI.

Gavaud, M., Muller, J.P. & Fromaget, M. 1976. Les étapes de l'évolution des sols dans les alluvions de la Bénoué (Nord-Cameroun). *Cahiers de l'ORSTOM. Série Pédologie.* **14,** 321–335.

Guis, R. 1976. Un bilan des travaux visant à la mise en culture des sols hardé du Nord-Cameroun. *Agronomie Tropicale.* **31,** 141–158.

Jamagne, M., De Coninck, F., Robert, M. & Maucorps, J. 1984. Mineralogy of clay fractions of some soils on loess in Northern France. *Geoderma,* **33,** 319–342.

Kooistra, M.J. & Tovey, N.K. 1994. Effects of compaction on soil microstructure. In: *Soil Compaction in Crop Production* (eds B.D. Soane and C. van Ouwerkerk), pp. 91–111. Elsevier Science, Amsterdam.

Lamotte, M. 1995. *Les sols à très forte cohésion des zones tropicales arides. Etude du hardé Lagadgé au Nord-Cameroun.* Collection TDM, ORSTOM, Paris.

Lamotte, M., Bruand, A., Dabas, M., Donfack, P., Gabalda, G., Hesse, A., Humbel, F.X. & Robain, H. 1994. Distribution d'un horizon à forte cohésion au sein d'une couverture de sol aride du Nord-Cameroun: apport d'une prospection électrique. *Comptes Rendus de l'Académie des Sciences de Paris. Série II,* **318,** 961–968.

Lamotte, M., Bruand, A., Ohnenstetter, D., Ildefonse, P. & Pédro, G. 1997. A hard sandy-loam soil from semi-arid Northern Cameroon: II. Geochemistry and mineralogy of the bonding agent. *European Journal of Soil Science,* **48,** 227–237.

Lindbo, D.L., Rhoton, F.E., Bigham, J.M., Hudnall, W.H., Jones, F.S., Smeck, N.E. & Tyler, D.D. 1994. Bulk density and fragipan identification in loess soils of the lower Mississippi river valley. *Soil Science Society of America Journal,* **58,** 884–891.

Lozet, J.M. & Herbillon, A.J. 1971. Fragipan soils of Condroz (Belgium). Mineralogical, chemical and physical aspects in relation with their genesis. *Geoderma,* **5,** 325–343.

McKeague, J.A. & Wang, C. 1980. Micromorphology and energy dispersive analysis of ortstein horizons of podzolic soils from New Brunswick and Nova Scotia, Canada. *Canadian Journal of Soil Science,* **60,** 9–21.

Miller, F.P., Holowaychuk, N. & Wilding, L.P. 1971*a*. Canfield silt loam, a fragiudalf. I. Macromorphological, physical and chemical properties. *Soil Science Society of America Proceedings,* **35,** 319–324.

Miller, F.P., Wilding, L.P. & Holowaychuk, N. 1971*b*. Canfield silt loam, a fragiudalf. II. Micromorphology, physical and chemical properties. *Soil Science Society of America Proceedings,* **35,** 324–331.

Olson, K.R. 1985. Identification of fragipans by means of mercury intrusion porosimetry. *Soil Science Society of America Journal,* **49,** 406–409.

Payton, R.W. 1992. Fragipan formation in argillic brown earths (Fragiudalfs) of the Milfield Plain, north-east England: I. Evidence for a periglacial stage of development. *Journal of Soil Science,* **43,** 621–644.

Payton, R.W. 1993*a*. Fragipan formation in argillic brown earths (Fragiudalfs) of the Milfield Plain, north-east England: II. Post Devensian developmental processes and the origin of fragipan consistence. *Journal of Soil Science,* **44,** 703–723.

Payton, R.W. 1993*b*. Fragipan formation in argillic brown earths (Fragiudalfs) of the Milfield Plain, north-east England: III. Micromorphological SEM EDXRA studies of fragipan degradation and the development of glossic features. *Journal of Soil Science,* **44,** 725–739.

Seiny-Boukar, L., Floret, C. & Pontanier, R. 1992. Degradation of savanna soils and reduction of water available for the vegetation. The case of northern Cameroon vertisols. *Canadian Journal of Soil Science,* **72,** 481–488.

Singer, J.K., Anderson, J.B., Ledbetter, M.T., McCave, I.N., Jones, K.P.N. & Wright, R. 1988. An assessment of analytical techniques for the size analysis of fine-grained sediments. *Journal of Sedimentology and Petrology,* **58,** 534–543.

Smeck, N.E. & Ciolkosz, E.J. (eds) 1989. *Fragipans: Their Occurrence, Classification and Genesis*, Soil Science Society of America, Special Publication No 24, Madison, WI.

Soil Survey Division Staff 1993. *Soil Survey Manual.* US Government. Printing Office, United States Department of Agriculture Handbook, Washington, DC.

Witty, J.E. & Knox, E.G. 1989. Identification, role in Soil Taxonomy, and worldwide distribution of fragipans. In: *Fragipans: Their Occurrence, Classification and Genesis* (eds N.E. Smeck and E.J. Ciolkosz), pp. 1–9. Soil Science Society of America, Special Publication No 24, Madison, WI.